

Communication

Effects of Substitution on Solid-State Fluorescence in 9-Aryl-9-methyl-9*H*-9-silafluorenes

Yoshinori Yamanoi *, Takayuki Nakashima, Masaki Shimada, Hiroaki Maeda and Hiroshi Nishihara *

Department of Chemistry, School of Science, The University of Tokyo, 7-3-1 Hongo, Bunkyo-ku, Tokyo 113-0033, Japan; k-nakashima@chem.s.u-tokyo.ac.jp (T.N.); shimada@chem.s.u-tokyo.ac.jp (M.S.); h-maeda@chem.s.u-tokyo.ac.jp (H.M.)

* Correspondence: yamanoi@chem.s.u-tokyo.ac.jp (Y.Y.); nishihara@chem.s.u-tokyo.ac.jp (H.N.); Tel.: +81-3-5841-4347 (Y.Y.); +81-3-5841-4346 (H.N.); Fax: +81-5841-8063 (Y.Y. & H.N.)

Academic Editor: Mitsuo Kira

Received: 15 July 2016; Accepted: 31 August 2016; Published: 3 September 2016

Abstract: Aromatic groups were incorporated into 9*H*-9-silafluorene units at the 9-position (mono-9*H*-silafluorenes) and 9,9'-positions (di-9*H*-9-silafluorenes). The aryl substituents showed weak conjugation to the 9*H*-9-silafluorene for 9-aryl substituted ones 1–7 and a 9,9'-phenylene substituted one (compound 8) and they exhibited similar absorption and emission spectra. The 9*H*-9-silafluorene 10 containing a 5,5'-(2,2'-bithiophenyl) group showed a significantly red-shifted absorption and fluorescence maxima in the solid-state. Single-crystal X-ray diffraction studies found J-type aggregated structures formed by intermolecular CH– π interactions (ca. 2.6–2.7 Å). Density functional theory (DFT), time-dependent DFT (TD-DFT), and configuration interaction single (CIS) calculations were conducted to explain the observed optical properties.

Keywords: 9*H*-9-silafluorene; thiophene; UV absorption; solid-state emission; single-crystal X-ray diffraction; J-aggregation

1. Introduction

9*H*-9-Silafluorenes are attractive building blocks for fluorescent materials because of their appealing optical properties, high stability against light and chemical agents, and high quantum yields [1–4]. Extending the conjugated π -systems from the 9*H*-9-silafluorene units through the introduction of functional aromatic substituents can shift the absorption/emission maxima to longer wavelengths, and fine-tune the optoelectronic properties. Therefore, the modification and development of 9*H*-9-silafluorenes have been actively investigated. Introducing functional groups on the 9*H*-9-silafluorene ring is an established way to lengthen the π -conjugation system and tune the HOMO–LUMO gaps, and thus essential for the full control of electronic and optical properties [5–8]. However, despite the interest in 9*H*-9-silafluorenes, their chemistry has not been investigated extensively for the molecular design of fluorescent materials. In particular, there are very few reports on systematic modification with aromatic compounds at the 9-position [9,10].

To obtain emitter molecules with improved photoluminescence properties, we developed a series of 9*H*-9-silafluorene derivatives combined with aromatic rings at the 9-position and investigated their influence on physical properties. The scarcity of prior works reporting functionalization at the 9-position of 9*H*-9-silafluorenes is likely due to the lack of an appropriate synthetic method. Recent developments have suggested that transition-metal-catalyzed arylation of hydrosilane is effective for preparing 9*H*-9-silafluorene-based π -conjugated functional materials, and may facilitate their use as fluorescent materials [11–15]. Our group has been designing and synthesizing silicon-bridged biaryl compounds and investigating their photochemical properties in solution and

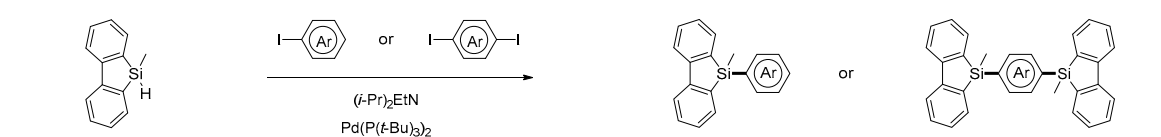
in the solid state [16,17]. As part of this endeavor, this work reports the synthesis and photophysical properties of a series of 9-aryl-9-methyl-9H-9-silafluorenes. Their structure-property relationships are explored through crystallographic analysis and theoretical calculations.

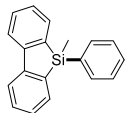
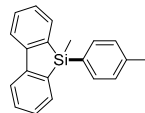
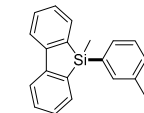
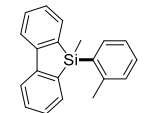
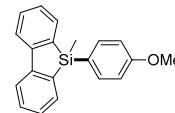
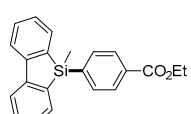
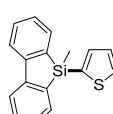
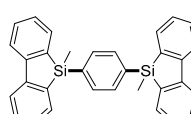
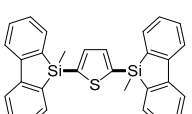
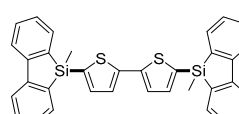
2. Results and Discussion

2.1. Synthesis and Characterization

The modified 9H-9-silafluorene derivatives **1–10** (Table 1) were prepared by the Pd-promoted arylation of 9-methyl-9H-9-silafluorene [18,19] with aryl iodides in THF using diisopropylethylamine as a base. After an appropriate workup, the derivatives were obtained in up to 56% yield. The reaction worked for both electron-rich (compounds **2–5**) and electron-poor aryl iodides (compound **6**). Reactive functional groups, such as an ester substituent, were compatible with the reaction conditions (compound **6**). 1,4-Diiodobenzene, 2,5-diiodothiophene, and 5,5'-diiodo-2,2'-bithiophene were also used in the arylation of 9-methyl-9H-9-silafluorene to give 1:2 coupled products **8–10**. Compounds **1**, **3** and **5–10** were solids and all compounds were soluble in common organic solvents. The resulting chromophores were characterized by $^1\text{H-NMR}$, $^{13}\text{C}\{^1\text{H}\}\text{-NMR}$, and HRMS spectroscopies, and were found to be consistent with the proposed structures. Compounds **1**, **3** and **5–10** are stable in the solid state, and could be stored without any special precautions.

Table 1. Structures and yields of 9H-9-silafluorenes **1–10**^a.



				
1 (41%) ^b	2 (24%) ^b	3 (35%) ^b	4 (56%) ^b	5 (39%) ^b
				
6 (28%) ^b	7 (37%) ^b	8 (11%) ^c	9 (13%) ^c	10 (17%) ^c

^a Numbers in parentheses are isolated yield. *Reagents and Conditions:* ^b Iodoarene (1.0 mmol), 9-methyl-9H-9-silafluorene (2.0 mmol), and triethylamine (3.0 mmol), Pd(P(*t*-Bu)₃)₂ (0.05 mmol), THF (1.0 M), 1 day, under Ar. ^c Iodoarene (2.0 mmol), 9-methyl-9H-9-silafluorene (1.0 mmol), and triethylamine (6.0 mmol), Pd(P(*t*-Bu)₃)₂ (0.05 mmol), THF (1.0 M), 1 day, under Ar.

2.2. Absorption and Emission Spectra

Optical properties were investigated by UV-vis and fluorescence spectroscopy. The absorption maxima λ_{abs} , emission maxima λ_{em} , fluorescence quantum yields ϕ , and fluorescence lifetimes τ are listed in Table 2. Figures S1–S4 (see Supplementary Materials) show the compounds' absorption and emission spectra in degassed *n*-hexane at room temperature. Despite the different aromatic groups at the 9-position, the absorption and emission spectra showed no major differences for **1–8** in solution and in the solid state. The electronic absorption spectra contained two peaks at ca. 288 nm and ca. 277 nm, corresponding to the π - π^* transition of the 9H-9-silafluorene fluorophore. The absorption coefficients of **8–10**, which have double 9H-9-silafluorene rings, were larger than those of **1–7**. The lowest-energy absorptions of **10** showed a bathochromic shift relative to those of **1–9**, indicating that the substituent

at the 9-position was conjugated with the 5,5'-(2,2'-bithiophenyl) groups. The fluorescence spectra recorded in *n*-hexane showed an emission band at around 340 nm, and appeared similar for all compounds except **10**, whose fluorescence band was red-shifted to 390 nm. The single fluorescence peak suggested that the emission occurred from only the lowest excited state. All the chromophores displayed fluorescence quantum yields of $\phi = \text{ca. } 0.1$ in *n*-hexane, consistent with values previously reported for 9*H*-9-silafluorenes [20–22].

Table 2. Photophysical properties of 9*H*-9-silafluorene derivatives **1–10** ^a.

Compound	In <i>n</i> -Hexane					In the Solid State			
	λ_{abs} (nm) ^b	ϵ ($10^4 \text{ M}^{-1} \cdot \text{cm}^{-1}$)	λ_{em} (nm) ^c	Φ ^d	τ (ns) ^e	λ_{ex} (nm)	λ_{em} (nm) ^c	Φ ^d	τ (ns)
1	<u>277</u> , 287	1.10	342	0.08	4.0	320	346	0.05	7.2 ^e
2	<u>277</u> , 288	1.10	340	0.10	3.9	- ^f	- ^f	- ^f	- ^f
3	<u>278</u> , 289	1.73	341	0.07	3.7	324	345	0.18	7.2 ^e
4	<u>278</u> , 289	1.39	341	0.14	4.0	- ^f	- ^f	- ^f	- ^f
5	<u>280</u> , 288	1.66	340	0.04	3.8	321	344	0.18	7.8 ^e
6	<u>277</u> , 288	1.24	343	0.09	3.9	326	348	0.18	7.7 ^e
7	<u>277</u> , 288	1.16	344	0.07	3.6	323	347, 385	0.11	3.3, 0.9 ^e
8	<u>277</u> , 289	2.25	342	0.12	3.8	321	345	0.11	4.4 ^e
9	<u>264</u> , <u>277</u> , 289	3.31	348, 490 ^g	0.07	2.3	444	500	0.20	0.5 ^h
10	279, <u>323</u>	2.54	390, 505 ⁱ	0.04	0.6	446	524	0.06	0.6 ^h

^a All measurements were carried out at rt. ^b Maximum absorption wavelength. Underlined values are wavelengths with the highest peak intensity. ^c Maximum fluorescence wavelength at λ_{abs} or λ_{ex} . ^d Absolute fluorescent quantum yield measured with an integrating sphere. ^e Fluorescence lifetime measured by photoexcitation at 280 nm. ^f Compounds obtained as oils. ^g Excited at 406 nm. ^h Fluorescence lifetime measured by photoexcitation at 406 nm. ⁱ Excited at 403 nm.

Compounds **1–8** emitted in the UV-A region with little change in luminescence properties between the solution and the solid state. The nature of the arenyl moiety of the 1:2 coupling products (compounds **9** and **10**) affected the solid state emission considerably (Figure 1). Compounds **1–8** emitted in the UV-A range in the solid state, and showed little difference between the solid state and solution spectra like compounds **1–7**. The 1:2 coupling products containing a thiophene ring (compound **9**) or a 2,2'-bithiophene ring (compound **10**) had their maximum fluorescence at visible wavelengths (500 nm) with a bathochromic shift of 127 nm relative to the maxima for chromophores **1–8**. The fluorescence spectra of **9** (excited at 406 nm) and **10** (excited at 403 nm) in solution displayed red-shifted emission due to the partial solid state-type emission at higher concentration (Figure S5). Fluorescence properties in the solid state are determined by molecular packing in addition to the molecular structure, with aggregation affecting both spectroscopic and photophysical properties. The emissions of **9** and **10** showed slightly higher quantum yield in the solid state than that in solution. They also showed short lifetimes of ca. 0.5 ns, similar to previous reports [23,24]. These results are attributed to the difference in the solid state structure and indicated the formation of J-aggregation. The molecular packing in the solid state was examined using single-crystal X-ray diffraction analysis.

2.3. Thermal Stability

To investigate the thermal stability, thermogravimetric and differential thermal analysis (TG-DTA) for **7–10** were carried out under a nitrogen atmosphere. Clearly, thermal properties of these compounds were determined by their chemical structures. From the TG-DTA curves shown in Figure S8, mono-9*H*-9-silafluorene **7** remains unchanged upon heating to 200 °C and is decomposed at over 220 °C. On the other hand, aryl-bridged di-9*H*-9-silafluorenes **8** and **9** are thermally stable up to 320 °C and 310 °C (Figures S9 and S10). The highest thermal stability of compound **10** was revealed by the almost constant TG (less than 5% weight loss) up to 360 °C (Figure S11). These results indicated that modified 9*H*-9-silafluorenes displayed high thermal stability, especially aryl-bridged di-9*H*-9-silafluorenes.

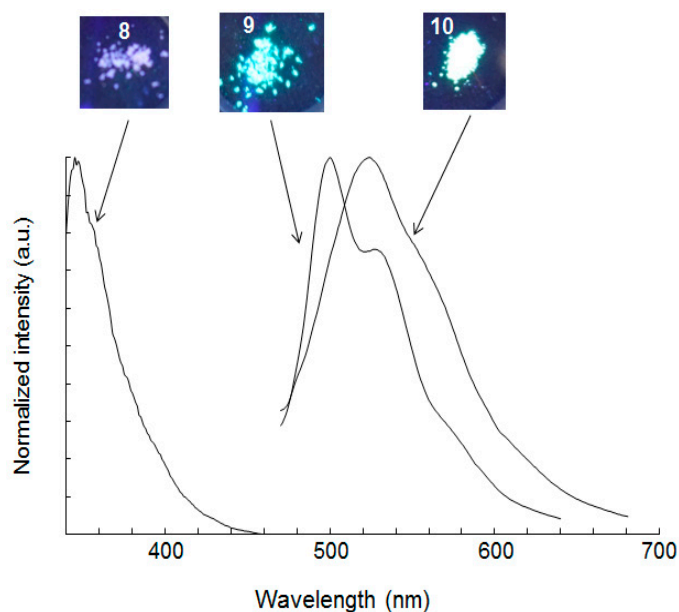


Figure 1. Images of luminescence under UV irradiation and fluorescence spectra of compounds **8–10** in the solid state.

2.4. X-ray Analysis

Single crystals are widely used to study molecular structures, molecular packing, and intermolecular interactions. Single crystals of **8–10** were analyzed to explain the red-shifted emissions in crystalline **9** and **10**. The structures and molecular packing were confirmed by X-ray crystallographic analysis (Figure 2) [25].

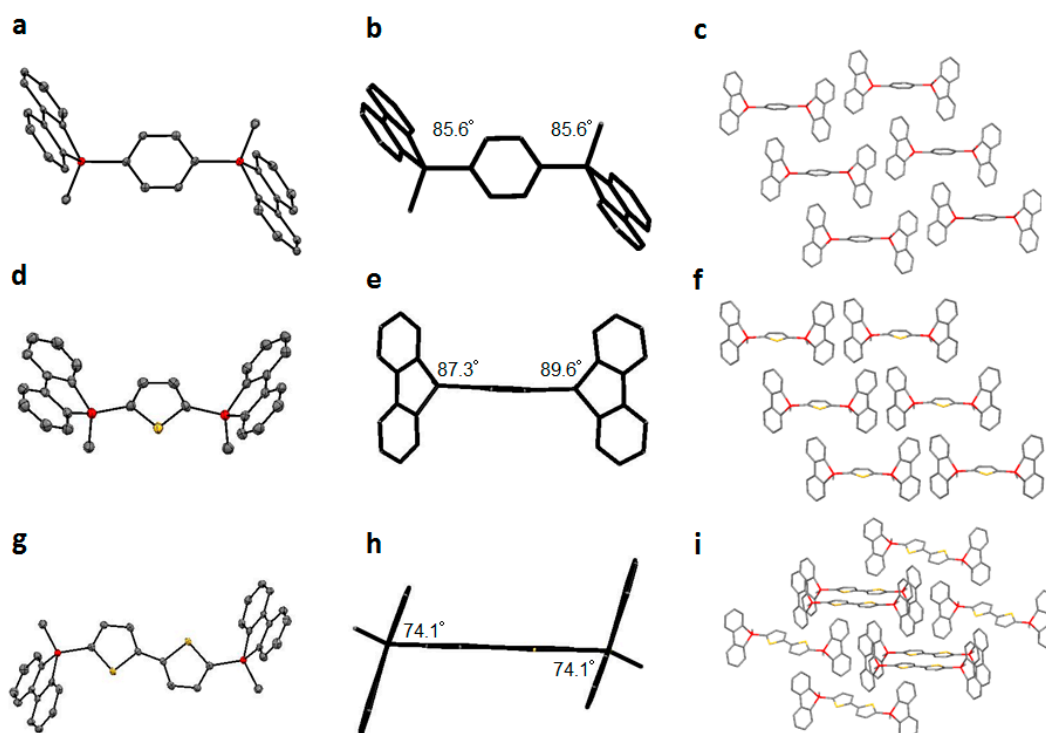


Figure 2. (a,d,g) ORTEP drawings (50% probability ellipsoids), (b,e,h) the angle between siloles and center aryl groups, and (c,f,i) packing structures of (a,b,c) **8**, (d, e, f) **9**, and (g,h,i) **10**. Hydrogen atoms are omitted for clarity.

The Si–C bond lengths were ca. 1.8–1.9 Å, similar to the standard Si–C length previously reported for 9*H*-9-silafluorenes. The 9*H*-9-silafluorene moieties appeared almost flat with deformation of the silicon atom from the ideal geometry of sp³ silicon. Compounds **8** and **10** had an *anti* conformation, whereas compound **9** had a *syn* conformation in the solid state. The two thiophenes of **10** were ideally coplanar with a 180° torsion angle, which allowed dense molecular packing. The dihedral angles between the central aryl plane and the 9*H*-9-silafluorene plane are shown in Figure 2. The 9*H*-9-silafluorenes **8** and **9** were positioned almost perpendicular to the central aromatic ring. However, the dihedral angles of **10** between the central bithiophene ring and each 9*H*-9-silafluorene moieties were ca. 74°. These dihedral angles suggest effective σ*–π* conjugation between these planes, especially in compound **9**.

The packing type and interactions strongly affect the solid-state emission. The crystal packing of **8–10** had a one-dimensional columnar structure. Their central phenyl or thiophene groups acted on the peripheral 9*H*-9-silafluorene rings by an edge-to-face CH–π interaction with a separation of 2.6–2.7 Å. The shortest distance between the π-planes of adjacent molecules was 6–7 Å. These compounds showed no ring–ring stacking interactions—which cause luminescence quenching—owing to the steric effects of the central aryl group at the 9,9'-position of 9*H*-9-silafluorene.

2.5. Theoretical Modeling

To gain more in depth insight into the electronic properties of the target chromophores, DFT, TD-DFT, and CIS calculations were conducted with the Gaussian 09 program using the B3LYP functional and 6-31G* basis set [26]. Figure 3 displays their optimized molecular structures together with the frontier molecular orbital profiles of **1**, **8**, **9**, and **10** as representative compounds. The calculated results are in good agreement with the experimental observation. Figure 3 shows that HOMOs of **1** and **8** are located on the 9*H*-9-silafluorene moiety and no lobe is spread over the phenyl ring at 9- and 9,9'-positions. LUMOs of **1** and **8** are localized on 9*H*-9-silafluorene and silicon bridges. Accordingly, **1** and **8** provided the π–π* transition of 9*H*-9-silafluorene unit in the lowest energy excitation.

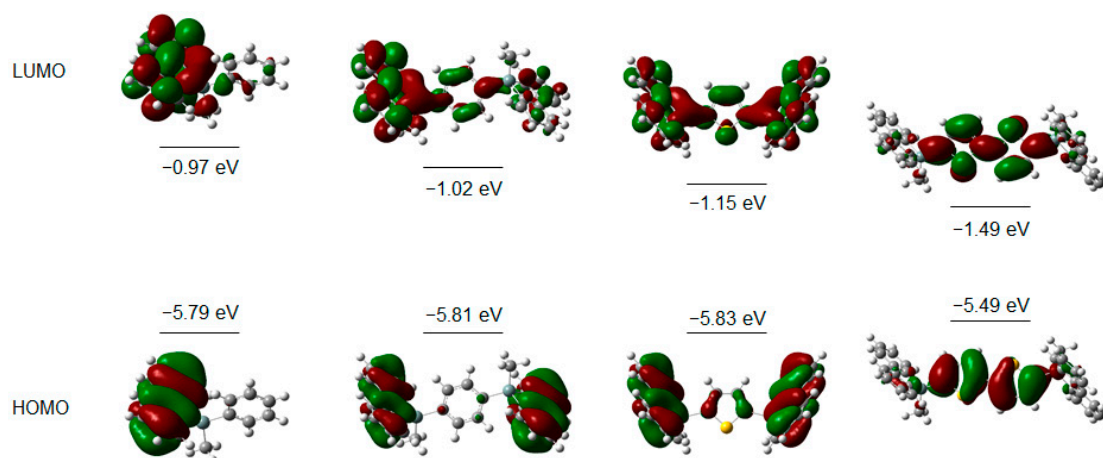


Figure 3. HOMO and LUMO diagrams and calculated energy levels for **1**, **8**, **9**, and **10** (left to right).

In contrast, the LUMO of **9** is spread over the whole molecule and is stabilized by σ*–(Si–C)–π* conjugation in comparison with **1** and **8**. The HOMO and LUMO of **10** are predominantly located on the central 2,2'-bithiophene moiety. The HOMO–LUMO energy gap was decreased in the order of benzene, thiophene, 9*H*-9-silafluorene, and 2,2'-bithiophene. Therefore, the 9*H*-9-silafluorene functionality plays a dominant role in HOMO and LUMO of **1**, **8**, and **9**. The 2,2'-bithiophene moiety in **10** causes the HOMO and LUMO to be localized mainly on the central 2,2'-bithiophene group. Their LUMO energy levels are lower than **1**, whereas the HOMO energies are similar. The energy gap between the HOMO

and LUMO gradually decreases in the order of **1** (4.82 eV), **8** (4.79 eV), **9** (4.68 eV), and **10** (4.00 eV). The conjugation of the thiophene groups greatly reduces the HOMO–LUMO energy gap. These calculated results are consistent with the observed bathochromic shift of the lowest-energy absorption wavelength in the UV spectra. The absorption peak of **10** at 323 nm was significantly red-shifted relative to those of the other compounds. The DFT calculations suggest that the longest absorption band of **10** arises from the π – π^* transition around the bithiophene ring. The decrease of the HOMO–LUMO energy gap should also affect the emission spectra substantially. The observed spectra suggest that UV-emitting compounds can be tuned with aryl substitution at the 9-position of 9H-9-silafluorenes; the subsequent large red shift can lead to a blue–green emission.

Moreover, the dipole moment and transition dipole moment of **8–10** were estimated utilizing CIS calculation. The 1,4-phenylene substituent (compound **8**) does not affect the dipole moment (0.05 D) and transition dipole moment (0.08 D), whereas **9** and **10** displayed larger dipole moments (0.52 D for **9** and 0.36 D for **10**) and transition dipole moments (0.25 D for **9** and 10.76 D for **10**), indicative of J-type aggregation in the solid state. The X-ray crystallography results, dipole-dipole interactions, and photophysical properties of **9** and **10** suggested J-aggregation, which accounted for the improved solid-state efficiency and red-shifted fluorescence spectra [27].

3. Experimental Section

3.1. General Information

All reactions were carried out under an argon atmosphere. All chemicals were purchased from commercial sources and used without further purification unless otherwise noted. 9-Methyl-9H-9-silafluorene was synthesized according to the literature [17,18]. Solvents used obtained from a solvent purification system. Melting points were measured with a Yanaco Micro Melting Point apparatus (Yanaco, Tokyo, Japan) and are uncorrected. ^1H - and $^{13}\text{C}\{^1\text{H}\}$ -NMR spectra were recorded on a US-500 spectrometer (Bruker corporation, Billerica, MA, USA) at 500 and 125 MHz, respectively. GC-MS spectra were recorded with a GC-MS-QP2010 spectrometer (Shimadzu, Tokyo, Japan). FAB mass spectra were measured with a MStation JMS-700 spectrometer (JEOL Ltd., Tokyo, Japan). Absorption spectra were measured with a JASCO V-570 spectrometer (JASCO, Tokyo, Japan). Fluorescence spectra were measured with a F-4500 spectrometer (Hitachi, Tokyo, Japan). Fluorescent quantum yields were recorded with a C9920-02 spectrometer (Hamamatsu, Shizuoka, Japan) and determined with an integrating sphere. Fluorescence lifetimes were measured with a Hamamatsu C11367 spectrometer (Hamamatsu, Shizuoka, Japan). Preparative gel permeation chromatographic separation was carried out with a LC-9110 NEXT recycling preparative HPLC system (JAI, Tokyo, Japan). Thermogravimetric and differential thermal analysis (TG-DTA) were measured with a Thermoplus TG 8120 (Rigaku, Tokyo, Japan). All TG-DTA measurements were conducted under N_2 atmosphere with heating rate as $10\text{ }^\circ\text{C}/\text{min}$ and Al_2O_3 was used for reference. All calculations were performed at the B3LYP/6-31G* level to extract theoretical electronic properties and correlated with experimental trends.

3.2. Typical Experimental Procedure for the Preparation of **1–7**

Iodoarene (1.0 mmol), 9-methyl-9H-9-silafluorene (2.0 mmol), and triethylamine (3.0 mmol) were added to a solution of $\text{Pd}(\text{P}(t\text{-Bu})_3)_2$ (0.05 mmol) in THF (1.0 M). The reaction mixture was stirred at room temperature for 1 day under argon, and then quenched with water. The aqueous layer was extracted with dichloromethane three times and dried over sodium sulfate. The solvent was removed in vacuo, and the residue was purified by column chromatography to afford the desired mono arylated 9H-9-silafluorenes. Analytically pure compounds were isolated by purification with GPC or recrystallization.

3.3. Typical Experimental Procedure for the Preparation of 8–10

Diiodoarene (2.0 mmol), 9-methyl-9H-9-silafluorene (1.0 mmol), and triethylamine (6.0 mmol) were added to a solution of Pd(P(*t*-Bu)₃)₂ (0.05 mmol) in THF (1.0 M). The reaction mixture was stirred at room temperature for 1 day under argon, and then quenched with water. The aqueous layer was extracted with dichloromethane three times and dried over sodium sulfate. The solvent was removed in vacuo, and the residue was purified by column chromatography to afford the desired di-arylated 9H-9-silafluorenes. Analytically pure compounds were isolated by purification with GPC or recrystallization.

3.4. X-ray Crystallography

X-ray diffraction data for **8** were collected at 93 K on a Rigaku Saturn 724 (Rigaku, Tokyo, Japan) diffractometer with multi-layer mirror monochromated Mo K α radiation ($\lambda = 0.71075 \text{ \AA}$). X-ray diffraction data of **9** and **10** were collected at 113 K with an AFC10 (Rigaku, Tokyo, Japan) diffractometer coupled with a Rigaku Saturn CCD system equipped with a rotating-anode X-ray generator producing graphite monochromated Mo K α ($\lambda = 0.71070 \text{ \AA}$) radiation. Lorentz-polarization and empirical absorption corrections were performed with the program Crystal Clear 2.0 (Rigaku, Tokyo, Japan) (**8**) or Crystal Clear 1.3.6 (Rigaku, Tokyo, Japan) (**9** and **10**). The structures were solved by the direct method using SIR-92 program [28], and refined by the full-matrix least-squares techniques against F^2 implementing SHELXL-97 [29,30].

3.5. Physical Data of 1–10

9-Methyl-9-phenyl-9H-9-silafluorene (**1**) [18,19]. Yield: 41%. Colorless solid. ¹H-NMR (CDCl₃) δ 7.86 (d, 2H, $J = 7.6$ Hz), 7.65 (d, 2H, $J = 6.9$ Hz), 7.55 (d, 2H, $J = 6.7$ Hz), 7.45 (t, 2H, $J = 7.7$ Hz), 7.38–7.26 (m, 5H), 0.73 (s, 3H). ¹³C{¹H}-NMR (CDCl₃) δ 148.4 (C_q), 137.4 (C_q), 134.6 (C_q), 134.5 (CH), 133.4 (CH), 130.5 (CH), 129.8 (CH), 128.1 (CH), 127.6 (CH), 121.0 (CH), -5.0 (CH₃). EI-MS m/z 272 [M]⁺.

9-Methyl-9-(*p*-tolyl)-9H-9-silafluorene (**2**). Yield: 24%. Colorless oil. ¹H-NMR (CDCl₃) δ 7.85 (d, 2H, $J = 7.6$ Hz), 7.63 (dd, 2H, $J = 6.3$ Hz, 3.0 Hz), 7.44–7.42 (m, 3H), 7.27 (td, 2H, $J = 7.3$ Hz, 0.6 Hz), 7.13 (d, 2H, $J = 7.6$ Hz), 2.34 (s, 3H), 0.71 (s, 3H). ¹³C{¹H}-NMR (CDCl₃) δ 148.4 (C_q), 139.9 (C_q), 137.7 (C_q), 134.6 (CH), 133.4 (CH), 130.9 (C_q), 130.4 (CH), 128.9 (CH), 127.6 (CH), 121.0 (CH), 21.6 (CH₃), -5.0 (CH₃). EI-MS m/z 286 [M]⁺. HRMS (FAB) m/z [M + H]⁺ Calcd for C₂₀H₁₉Si 287.1256; found 287.1241.

9-Methyl-9-(*m*-tolyl)-9H-9-silafluorene (**3**). Yield: 33%. Colorless solid. Mp: 108.8–110.3 °C. ¹H-NMR (CDCl₃) δ 7.87 (d, 2H, $J = 7.6$ Hz), 7.68–7.64 (m, 3H), 7.49 (td, 2H, $J = 7.6$ Hz, 1.3 Hz), 7.31–7.25 (m, 3H), 7.18 (t, 1H, $J = 7.4$ Hz), 7.11 (d, 1H, $J = 7.3$ Hz), 2.15 (s, 3H), 0.73 (s, 3H). ¹³C{¹H}-NMR (CDCl₃) δ 148.1 (C_q), 144.9 (C_q), 137.9 (C_q), 136.0 (CH), 133.4 (CH), 132.9 (C_q), 130.3 (CH), 130.2 (CH), 129.8 (CH), 127.6 (CH), 125.1 (CH), 121.1 (CH), 22.8 (CH₃), -3.6 (CH₃). EI-MS m/z 286 [M]⁺. HRMS (FAB) m/z [M + H]⁺ Calcd for C₂₀H₁₉Si 287.1256; found 287.1241.

9-Methyl-9-(*o*-tolyl)-9H-9-silafluorene (**4**). Yield: 56%. Colorless oil. ¹H-NMR (CDCl₃) δ 7.86 (d, 2H, $J = 7.9$ Hz), 7.65 (d, 2H, $J = 7.6$ Hz), 7.45 (td, 2H, $J = 7.6$ Hz, 1.3 Hz), 7.36 (m, 2H), 7.27 (td, 2H, $J = 7.3$ Hz, 0.9 Hz), 7.23–7.17 (m, 2H), 2.29 (s, 3H), 0.72 (s, 3H). ¹³C{¹H}-NMR (CDCl₃) δ 148.4 (C_q), 137.6 (C_q), 137.5 (C_q), 135.0 (CH), 134.4 (C_q), 133.4 (CH), 131.6 (CH), 130.8 (CH), 130.5 (CH), 128.0 (CH), 127.6 (CH), 121.0 (CH), 21.5 (CH₃), -4.9 (CH₃). EI-MS m/z 286 [M]⁺. HRMS (FAB) m/z [M + H]⁺ Calcd for C₂₀H₁₉Si 287.1256; found 287.1241.

9-(*p*-Methoxyphenyl)-9-methyl-9H-9-silafluorene (**5**). Yield 39%. Colorless solid. Mp: 88.5–90.0 °C. ¹H-NMR (CDCl₃) δ 7.86 (d, 2H, $J = 7.6$ Hz), 7.62 (d, 2H, $J = 7.6$ Hz), 7.48–7.42 (m, 4H), 7.26 (t, 2H, $J = 6.8$ Hz), 6.87 (d, 2H, $J = 8.8$ Hz), 3.77 (s, 3H), 0.70 (s, 3H). ¹³C{¹H}-NMR (CDCl₃) δ 161.2 (C_q), 148.3 (C_q), 137.8 (C_q), 136.0 (CH), 133.3 (CH), 130.4 (CH), 127.6 (CH), 125.2 (C_q), 120.9 (CH), 113.9 (CH), 55.1 (CH₃), -4.9 (CH₃). EI-MS m/z 302 [M]⁺. HRMS (FAB) m/z [M]⁺ Calcd for C₂₀H₁₈OSi 302.1127; found 302.1115.

Ethyl 4-(9-methyl-9H-9-silafluoren-9-yl)benzoate (6). Yield: 28%. Colorless solid. Mp: 101.3–102.5 °C. $^1\text{H-NMR}$ (CDCl_3) δ 7.97 (d, 2H, $J = 8.2$ Hz), 7.87 (d, 2H, $J = 7.7$ Hz), 7.64–7.61 (m, 4H), 7.47 (td, 2H, $J = 7.6$ Hz, 1.3 Hz), 7.29 (t, 2H, $J = 7.1$ Hz), 4.35 (q, 2H, $J = 8.3$ Hz), 1.36 (t, 3H, $J = 7.1$ Hz), 0.76 (s, 3H). $^{13}\text{C}\{^1\text{H}\}$ -NMR (CDCl_3) δ 166.6 (C_q), 148.5 (C_q), 140.9 (C_q), 136.7 (C_q), 134.4 (CH), 133.4 (CH), 131.6 (C_q), 130.8 (CH), 128.8 (CH), 127.8 (CH), 121.1 (CH), 61.0 (CH_2), 14.3 (CH_3), -5.2 (CH_3). EI-MS m/z 344 [M] $^+$. HRMS (FAB) m/z [M] $^+$ Calcd for $\text{C}_{22}\text{H}_{20}\text{O}_2\text{Si}$ 344.1236; found 344.1210.

9-Methyl-9-(thiophen-2-yl)-9H-9-silafluorene (7). Yield: 37%. Colorless solid. Mp: 70.3–71.5 °C. $^1\text{H-NMR}$ (CDCl_3) δ 7.84 (d, 2H, $J = 7.9$ Hz), 7.67 (d, 2H, $J = 7.2$ Hz), 7.62 (dd, 1H, $J = 4.7$ Hz, 1.0 Hz), 7.46 (td, 2H, $J = 7.5$ Hz, 1.4 Hz), 7.34 (dd, 1H, $J = 3.5$ Hz, 1.0 Hz), 7.28 (td, 2H, $J = 7.3$ Hz, 1.0 Hz), 7.17 (dd, 1H, $J = 4.6$ Hz, 3.2 Hz), 0.77 (s, 3H). $^{13}\text{C}\{^1\text{H}\}$ -NMR (CDCl_3) δ 148.1 (C_q), 136.8 (C_q), 136.4 (CH), 133.4 (C_q), 133.3 (CH), 132.1 (CH), 130.8 (CH), 128.4 (CH), 127.7 (CH), 121.0 (CH), -3.6 (CH_3). EI-MS m/z 278 [M] $^+$. HRMS (FAB) m/z [M] $^+$ Calcd for $\text{C}_{17}\text{H}_{14}\text{SSi}$ 278.0585; found 278.0570.

1,4-Bis(9-methyl-9H-9-silafluoren-9-yl)benzene (8). Yield: 11%. Colorless solid. Mp: 193.2–194.5 °C. $^1\text{H-NMR}$ (CDCl_3) δ 7.83 (d, 4H, $J = 7.6$ Hz), 7.59 (d, 4H, $J = 6.6$ Hz), 7.49 (s, 4H), 7.43 (td, 4H, $J = 7.4$ Hz, 1.2 Hz), 7.24 (td, 4H, $J = 7.1$ Hz, 0.8 Hz), 0.69 (s, 6H). $^{13}\text{C}\{^1\text{H}\}$ -NMR (CDCl_3) δ 148.4 (C_q), 137.1 (C_q), 136.5 (C_q), 133.9 (CH), 133.3 (CH), 130.5 (CH), 127.6 (CH), 121.0 (CH), -5.3 (CH_3). EI-MS m/z 466 [M] $^+$. HRMS (FAB) m/z [M] $^+$ Calcd for $\text{C}_{32}\text{H}_{26}\text{Si}_2$ 466.1573; found 466.1591.

2,5-Bis(9-methyl-9H-9-silafluoren-9-yl)thiophene (9). Yield: 13%. Pale yellow solid. Mp: 179.5–181.0 °C. $^1\text{H-NMR}$ (CDCl_3) δ 7.83 (d, 4H, $J = 7.6$ Hz), 7.64 (d, 4H, $J = 7.0$ Hz), 7.44 (t, 4H, $J = 7.0$ Hz), 7.36 (s, 2H), 7.27 (t, 4H, $J = 7.3$ Hz), 0.7 (s, 6H). $^{13}\text{C}\{^1\text{H}\}$ -NMR (CDCl_3) δ 148.1 (C_q), 141.1 (C_q), 137.6 (CH), 136.7 (C_q), 133.4 (CH), 130.8 (CH), 127.8 (CH), 121.1 (CH), -3.5 (CH_3). EI-MS m/z 472 [M] $^+$. HRMS (FAB) m/z [M] $^+$ Calcd for $\text{C}_{30}\text{H}_{24}\text{SSi}_2$ 472.1137; found 472.1147.

5,5'-Bis(9-methyl-9H-9-silafluoren-9-yl)-2,2'-bithiophene (10). Yield: 17%. Yellow solid. Mp: 251.2–252.8 °C. $^1\text{H-NMR}$ (CDCl_3) δ 7.84 (d, 4H, $J = 7.6$ Hz), 7.66 (d, 4H, $J = 6.7$ Hz), 7.46 (td, 4H, $J = 7.6$ Hz, 1.3 Hz), 7.28 (td, 4H, $J = 7.6$ Hz, 0.7 Hz), 7.18 (d, 2H, $J = 3.5$ Hz), 7.17 (d, 2H, $J = 3.5$ Hz), 0.75 (s, 6H). $^{13}\text{C}\{^1\text{H}\}$ -NMR (CDCl_3) δ 148.1 (C_q), 143.7 (C_q), 137.2 (CH), 136.4 (C_q), 133.3 (CH), 130.9 (CH), 127.8 (CH), 125.6 (CH), 121.0 (CH), -3.9 (CH_3). EI-MS m/z 554 [M] $^+$. HRMS (FAB) m/z [M] $^+$ Calcd for $\text{C}_{34}\text{H}_{26}\text{S}_2\text{Si}_2$ 554.1015; found 554.0992.

4. Conclusions

We have designed and synthesized 9H-9-silafluorene derivatives with different aryl groups incorporated at the 9-position. These fluorophores were formed through Pd-catalyzed arylation of 9H-9-silafluorene and aryl iodides. Various aromatic substituents at the 9-position were compared. Compounds 1–8, with various substituents on the silicon atom, all showed similar UV–Vis and emission spectra. Compounds 9 and 10 showed different solid-state emissions when aggregated owing to the modulation of their intermolecular interactions. The fluorescence of 9 and 10 was characterized by a large Stokes shift. The thermal stabilities of 7–10 were investigated by TG-DTA measurement. These compounds remain unchanged upon heating to 200 °C (compound 7), 320 °C (compound 8), 310 °C (compound 9), and 360 °C (compound 10), respectively. Theoretical calculations showed that thiophenyl or bithiophenyl substitutions of 9H-9-silafluorene at the 9,9'-positions decreased the HOMO–LUMO energy gap. Consistent with the calculations, these two compounds showed red-shifted UV–vis and emission spectra compared with the other compounds.

The solid-state optical and photophysical properties of the compounds were primarily affected by their molecular packing and dipole–dipole interaction. Our method facilitated the J-aggregated formation of fluorophores via a simple chemical-group substitution. Intermolecular CH– π interactions in the crystal assisted the slipped–stacked arrangement, and strongly affected the solid-state emission. The hindrance of the rotation in the solid state yielded higher quantum yields. Given that the

substitution can be easily achieved by a Pd-catalyzed coupling reaction, this synthetic approach appears useful to extend and improve these molecules' fluorescent properties.

Supplementary Materials: Supplementary materials are available online at <http://www.mdpi.com/1420-3049/21/9/1173/s1>.

Acknowledgments: The present work was financially in part supported by CREST from JST, Tokyo Kasei Chemical Promotion Foundation, Nippon Sheet Glass Foundation for Materials Science and Engineering, Precise Measurement Technology Promotion Foundation, Grant-in-Aids for Scientific Research (C) (No. 15K05604), and Scientific Research on Innovative Areas "Molecular Architectonics: Orchestration of Single Molecules for Novel Functions" (area 2509, Nos. 26110505, 26110506, 16H00957, and 16H00958) from the Ministry of Education, Culture, Sports, Science, and Technology, Japan. X-ray diffraction of **8** was supported by "Nanotechnology Platform" (project No.12024046) of the Ministry of Education, Culture, Sports, Science and Technology (MEXT), Japan.

Author Contributions: Yoshinori Yamanoi and Hiroshi Nishihara conceived and designed the experiments, and wrote the paper; Takayuki Nakashima performed the experiments; Masaki Shimada and Hiroaki Maeda analyzed the data and commented on the manuscript.

Conflicts of Interest: The authors declare no conflict of interest.

References and Notes

1. Corey, J.Y. Siloles: Part 2: Silaindenes (Benzosiloles) and Silafluorenes (Dibenzosiloles): Synthesis, Characterization, and Applications. *Adv. Organomet. Chem.* **2011**, *59*, 181–328. [[CrossRef](#)]
2. Shimizu, M.; Hiyama, T. Silicon-bridged biaryls: Molecular design, new synthesis, and luminescence control. *Synlett* **2012**, *23*, 973–989. [[CrossRef](#)]
3. Zhang, Q.-W.; An, K.; He, W. Catalytic Synthesis of π -Conjugated Silole through Si–C (sp^3) Bond Activation. *Synlett* **2015**, *26*, 1145–1152.
4. Shimizu, M. Novel synthesis and luminescent properties of silicon-bridged biaryls. *J. Synth. Org. Chem. Jpn.* **2013**, *71*, 307–318. [[CrossRef](#)]
5. Fukazawa, A.; Yamaguchi, S. Ladder π -Conjugated Materials Containing Main-Group Elements. *Chem. Asian J.* **2009**, *4*, 1386–1400. [[CrossRef](#)] [[PubMed](#)]
6. Yamaguchi, S.; Xu, C.; Okamoto, T. Ladder π -Conjugated Materials with Main Group Elements. *Pure Appl. Chem.* **2006**, *78*, 721–730. [[CrossRef](#)]
7. Yamaguchi, S.; Xu, C. The Chemistry of Silicon-Containing Ladder π -Conjugated Systems. *J. Synth. Org. Chem. Jpn.* **2005**, *63*, 1115–1123. [[CrossRef](#)]
8. Yamaguchi, S.; Tamao, K. A Key Role of Orbital Interaction in the Main Group Element-Containing π -Electron Systems. *Chem. Lett.* **2005**, *34*, 2–7. [[CrossRef](#)]
9. Zhan, X.; Barlow, S.; Marder, S.R. Substituent effects on the electronic structure of siloles. *Chem. Commun.* **2009**, 1948–1955. [[CrossRef](#)] [[PubMed](#)]
10. Wang, D.; Liu, Q.; Yu, Y.; Wu, Y.; Zhang, X.; Dong, H.; Ma, L.; Zhou, G.; Jiao, B.; Wu, Z.; et al. Silafluorene moieties as promising building blocks for constructing wide-energy-gap host materials of blue phosphorescent organic light-emitting devices. *Sci. Chin. Chem.* **2015**, *58*, 993–998. [[CrossRef](#)]
11. Yamanoi, Y. Palladium-Catalyzed Silylations of Hydrosilanes with Aryl Halides Using Bulky Alkyl Phosphine. *J. Org. Chem.* **2005**, *70*, 9607–9609. [[CrossRef](#)] [[PubMed](#)]
12. Yamanoi, Y.; Taira, T.; Sato, J.-I.; Nakamura, I.; Nishihara, H. Efficient Preparation of Monohydrosilanes Using Palladium-Catalyzed Si–C Bond Formation. *Org. Lett.* **2007**, *9*, 4543–4546. [[CrossRef](#)] [[PubMed](#)]
13. Yamanoi, Y.; Nishihara, H. Efficient Synthesis of Arylsilanes by Cross-coupling of Aromatic Compounds with Hydrosilanes as Silicon Sources. *J. Synth. Org. Chem. Jpn.* **2009**, *67*, 778–786. [[CrossRef](#)]
14. Lesbani, A.; Kondo, H.; Yabusaki, Y.; Nakai, M.; Yamanoi, Y.; Nishihara, H. Integrated Palladium-Catalyzed Arylation of Heavier Group 14 Hydrides. *Chem. Eur. J.* **2010**, *16*, 13519–13527. [[CrossRef](#)] [[PubMed](#)]
15. Shimada, M.; Yamanoi, Y.; Nishihara, H. Unusual Reactivity of Group 14 Hydrides toward Organic Halides: Synthetic Studies and Application to Functional Materials. *J. Synth. Org. Chem. Jpn.* **2016**, *74*, in press.
16. Yabusaki, Y.; Ohshima, N.; Kondo, H.; Kusamoto, T.; Yamanoi, Y.; Nishihara, H. Versatile Synthesis of Blue Luminescent Siloles and Germoles and Hydrogen-Bond-Assisted Color Alteration. *Chem. Eur. J.* **2010**, *16*, 5581–5585. [[CrossRef](#)] [[PubMed](#)]

17. Nakashima, T.; Shimada, M.; Kurihara, Y.; Tsuchiya, M.; Yamanoi, Y.; Nishibori, E.; Sugimoto, K.; Nishihara, H. Fluorescence and phosphorescence of a series of silicon-containing six-membered-ring molecules. *J. Organomet. Chem.* **2016**, *805*, 27–33. [[CrossRef](#)]
18. Chang, L.S.; Corey, J.Y. Dehydrogenative Coupling of Diarylsilanes. *Organometallics* **1989**, *8*, 1885–1893. [[CrossRef](#)]
19. Becker, B.; Corriu, R.J.P.; Henner, B.J.L.; Wojnowski, W.; Peters, K.; von Schnering, H.G. Contributions to the chemistry of silicon-sulphur compounds: XLII. Bis(1-methyldibenzosilole)sulphide: Its synthesis, crystal structure, and reaction with chromium hexacarbonyl. *J. Organomet. Chem.* **1986**, *312*, 305–311. [[CrossRef](#)]
20. Cai, Y.; Samedov, K.; Dolinar, B.S.; Albright, H.; Guzei, I.A.; Hu, R.; Zhang, C.; West, R. Ring-Shaped Silafluorene Derivatives as Efficient Solid-State UV-Fluorophores: Synthesis, Characterization, and Photoluminescent Properties. *Chem. Eur. J.* **2014**, *20*, 14040–14050. [[CrossRef](#)] [[PubMed](#)]
21. Sanchez, J.C.; Trogler, W.C. Efficient blue-emitting silafluorene–fluorene-conjugated copolymers: Selective turn-off/turn-on detection of explosives. *J. Mater. Chem.* **2008**, *18*, 3143–3156. [[CrossRef](#)]
22. Puzstai, E.; Touloukhonova, I.S.; Temple, N.; Albright, H.; Zakai, U.I.; Guo, S.; Guzei, I.A.; Hu, R.R.; West, R. Synthesis and Photophysical Properties of Asymmetric Substituted Silafluorenes. *Organometallics* **2013**, *32*, 2529–2535. [[CrossRef](#)]
23. Maiti, N.C.; Mazumdar, S.; Periasamy, N. J- and H-Aggregates of Porphyrin-Surfactant Complexes: Time-Resolved Fluorescence and Other Spectroscopic Studies. *J. Phys. Chem. B* **1998**, *102*, 1528–1538. [[CrossRef](#)]
24. Venkatramaiyah, N.; Ramakrishna, B.; Venkatesan, R.; Pazb, F.A. A.; Tomé, J.P.C. Facile synthesis of highly stable BF₃-induced meso-tetrakis (4-sulfonato phenyl) porphyrin (TPPS₄)-J-aggregates: Structure, photophysical and electrochemical properties. *New J. Chem.* **2013**, *37*, 3745–3754. [[CrossRef](#)]
25. CCDC 1458152 (8), 1447977 (9) and 1447978 (10) contain the supplementary crystallographic data for this paper. These data can be obtained free of charge via <http://www.ccdc.cam.ac.uk/conts/retrieving.html> (or from the CCDC, 12 Union Road, Cambridge CB2 1EZ, UK; Fax: +44-1223-336033; E-mail: deposit@ccdc.cam.ac.uk).
26. Frisch, M.J.; Trucks, G.W.; Schlegel, H.B.; Scuseria, G.E.; Robb, M.A.; Cheeseman, J.R.; Scalmani, G.; Barone, V.; Mennucci, B.; Petersson, G.A.; et al. *Gaussian 09W*; Revision A.02 and Revision E.01; Gaussian, Inc.: Wallingford, CT, USA, 2009.
27. Kasha, M.; Rawls, H.R.; Ashraf El-Bayoumi, M. The exciton model in molecular spectroscopy. *Pure Appl. Chem.* **1965**, *11*, 371–392. [[CrossRef](#)]
28. Altomare, A.; Casciarano, G.; Giacovazzo, C.; Guagliardi, A.; Burla, M.C.; Polidori, G.; Camalli, M. SIR92—A program for automatic solution of crystal structures by direct methods. *J. Appl. Cryst.* **1994**, *27*, 435. [[CrossRef](#)]
29. Sheldrick, G.M. A short history of SHELX. *Acta Cryst.* **2008**, *A64*, 112–122. [[CrossRef](#)] [[PubMed](#)]
30. Sheldrick, G.M.; Schneider, T.R. [16] SHELXL: High-Resolution Refinement. *Methods Enzymol.* **1997**, *277*, 319–343. [[PubMed](#)]

Sample Availability: Samples of the compounds 1–10 are available from the authors.



© 2016 by the authors; licensee MDPI, Basel, Switzerland. This article is an open access article distributed under the terms and conditions of the Creative Commons Attribution (CC-BY) license (<http://creativecommons.org/licenses/by/4.0/>).